Nihon Reoroji Gakkaishi Vol.36, No.3, 125~131
(Journal of the Society of Rheology, Japan)

Article

Drag Reduction in the Flow of Aqueous Solutions of Detergent Through Mesh Screens

Keiko AMAKI*, Tomiichi HASEGAWA**, and Takatsune NARUMI**

*Department of Home Economics, Faculty of Education, Iwate University
3-18-33 Ueda, Morioka-shi, Iwate 020-8550, Japan
**Mechanical and Production Engineering, Faculty of Engineering, Niigata University
8050 Ikarashi-2nocho, Niigata-shi, Niigata 950-2181, Japan
(Received : September 25, 2007)

An experimental study was conducted on the flow of aqueous solutions of detergent through mesh screens to mimic cloth washing. Pressure losses across the mesh screens were measured for water, dilute polymer and several aqueous detergent solutions. A reduction of pressure losses was observed for the flow of aqueous solutions of low molecular weight surfactants such as Laurylether (AE), Laurylbenzene-sulfonic acid-sodiumsalt (LAS), Benzalkonium-chloride (BC) Sodium-dodecyl-sulfate (SDS), and Hexadecyltrimetyl-ammonium-bromide (CTAB), but not for the high molecular weight polymers like Polyethylene-oxide (PEO18) and Polyacrylamide (PAA), through mesh screens. A flow visualization experiment was carried out to observe the flow pattern upstream and downstream of the mesh screen. Photographic images revealed that, instead of an expected large converging flow from the upstream section into the screen opening as in orifice flow, the bulk of the liquid entering the screen aperture took the form of a liquid column of similar diameter as the inlet tube. Based on this observation, a flow model, which led to a new set of definitions of Reynolds number and drag coefficient, was proposed. Good correlations of drag coefficient and Reynolds number were obtained for all test solutions, and the drag reduction phenomenon was manifested for detergent aqueous solutions.
Key Words: Drag Reduction / Detergent / Surfactant / Mesh Screen / Drag Coefficient

1. INTRODUCTION

Excessive consumption of detergent in daily life is a major environmental concern. As a result, many industrial researches are aimed on better product formulation and effective usage of detergent. To date, most studies have been focused on the chemical effects of detergent, with very little attention on the effect of mechanical factors including the flow through fabric. Among the mechanical factors, the force of adhesion between submicron particles and substrate has been measured by Visser[1] using a shear flow device or an elect-osmotic flow device by Gotoh, et al.[2] Other factors such as the effects of shearing[3], bending and friction on clothes[4], as well as the penetrating flow of detergent through clothes[5,6] have also been investigated. Amaki, et al[7] measured the drag caused by solutions of low molecular surfactants (detergents) flowing over thin wires attached on a flat plate. The measured drag was found to be lower for low molecular detergents but higher for dilute polymer solutions than for water. Watanabe, et al[8] carried out a numerical analysis for this kind of flow using a viscoelastic constitutive equation and found that fluid elasticity decreased the drag only slightly but caused a huge reduction in lift. However, the effect of surfactant solutions on detergency is not clarified from a viewpoint of fluid mechanics yet.

In the present study, measurements of pressure drops are conducted on the flow of aqueous solutions of detergent through mesh screens, mimicking the flow behavior in cloth washing. Pressure losses are compared with those measured with water and dilute solutions of high molecular weight polymers. A flow model is proposed to explain the drag reduction phenomenon observed for detergent solutions. Finally we mention the kinematic effect of surfactant solutions in cloth washing.

2. EXPERIMENTAL

Figure 1 shows the detail of the experimental channels used. A mesh screen was spanned in the midst of the channel, normal to the flow direction, and the pressure differential as a function of flow rate was measured between upstream and downstream positions across the screen mesh using a pressure gauge (Tsukasa Sokken PZ-77, Japan). The average pressure error was found to be within ±5 %. The test channel was made of

acrylic plate, and was 300 mm long, 40 mm × 15 mm rectangular in cross section. Mesh screens were pasted over sectional apertures (15 mm × 15 mm, 10 mm × 10 mm rectangular, and 5 mm circular) drilled on a plate, and the plate was set in the test channel with packing. Pressure taps were set at 82 mm apart from the screen. The pressure differential Δp between the taps was measured and head loss h is defined as $h = \Delta p/(\rho g)$, where ρ is the density of liquid and g is the gravity acceleration.

A schematic diagram of the experimental apparatus is shown in Fig. 2. The test solution, stored in a tank of 2 m height, was made to flow through the test channel, and to discharge via a flow control valve. The flow rate was measured by weighing the liquid discharged over a time interval.

The test liquids used were ion exchange water, aqueous solutions of Polyethylene-oxide (PEO18) and Polyacrylamide (PAA), and various surfactants. These surfactants include Laurylether (AE(23)), Laurylbenzene-sulfonic acid-sodiumsalt (LAS), Hexadecyltrimetyl-ammonium-bromide (CTAB), Sodium-dodecyl-sulfate (SDS), and Benzalkonium-chloride (BC). The molecular weights and the solution concentrations of the test liquids are given in Table I.

Viscosities of the liquids η were measured using a capillary viscometer at room temperature. It can be seen in Fig. 3 that all tested liquids exhibit Newtonian behavior with viscosities of the order of 10^{-3} Pa•s, which is very close to that of water, within the experimental errors.

Two types of mesh screens were used: polyester and stainless threads. A photograph of the polyester mesh is shown in Fig. 4(a), where b is a side of mesh square. The screen mesh apertures S are either square of 15 mm × 15 mm and 10 × 10mm dimensions, or circular holes of diameter Φ 5 mm (Fig. 4(b)). Four kinds of thread numbers per inch, 230 ($b = 70$ μm), 255 ($b = 60$ μm), 270 ($b = 54$ μm) and 300 ($b = 45$ μm), were used as the polyester mesh; while 200 ($b = 87$ μm) threads per inch was used for the stainless mesh. The diameter of the mesh thread d was 40 μm for both polyester and stainless meshes.

Prior to the experiment for screen mesh flow, we tried to measure the pressure drops through the apertures without screen mesh, but those for the 15 mm and 10 mm square apertures were too small for measurement and data were obtained only for the Φ 5 mm aperture. The result showed that there was no discernible difference between water and the solutions used.

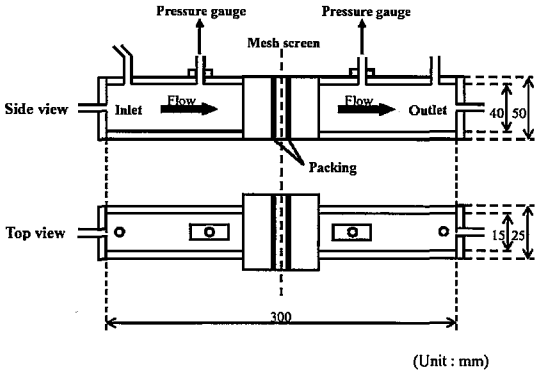

Fig. 1. Experimental method and the channel.

Table I. Molecular weight and concentration of the test materials.

Material	Molecular Weight	Concentration	
		Polyester Mesh	Stainless Mesh
PEO (18)	4.5×10^6	10ppm	-
PAA	3.4×10^6	10ppm	-
AE (23)	1214.5	0.01mol/L (1.2%)	0.5%
LAS	348.5	0.01mol/L (0.35%)	0.5%
CTAB	364.5	0.005mol/L (0.18%)	-
SDS	288.0	-	0.5%
BC	354.5	-	0.5%

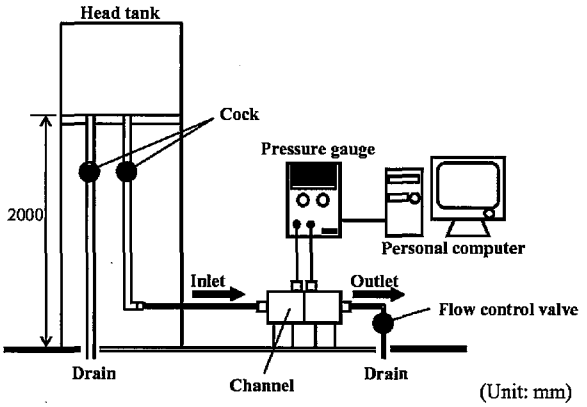

Fig. 2. Schema of the apparatus.

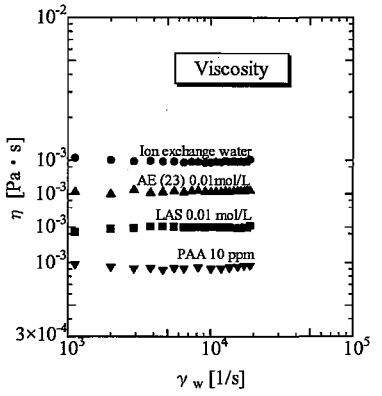

Fig. 3. Viscosity of the tested liquids η measured by a capillary viscometer. η is defined as the ratio of the wall shear stress to the wall shear rate γ_w. The temperature is 17-20 °C.

The velocity of the liquid flowing through the screen was calculated by dividing the measured flow rate by an effective flow area. For square openings, the velocity through the mesh V_m is given as

$$V_m = \frac{Q}{\alpha S} \tag{1}$$

where $\alpha = \frac{\sum b^2}{S}$ is the porosity, which represents the ratio of the effective pass area $\sum b^2$ in the mesh to the area of apertures S.

3. RESULTS AND DISCUSSION

Experimental results are presented in terms of head loss h as a function of strain rate V_m/b for all test liquids in Figs. 5(a-f), where cases A, B and C represents the size S of 15 mm × 15 mm, 10 mm × 10 mm, and Φ 5 mm respectively. It is evident that h is not a unique function of V_m/b, but depends slightly on the tread density and more strongly on the opening geometry and size. Consider the case for the flow through the 10 mm screen, as shown by Case B in Figs. 5(a)-(f), values of h correlate well with V_m/b only in the strain rate range of less than 2×10^3 sec^{-1} for water and the 10 ppm PEO solution (Figs. 5(a), (b)), but is extended to higher ranges of strain rate for other solutions. For instance, the correlation is extended to V_m/b up to 4×10^3 sec^{-1} for LAS and AE (23) (Figs. 5 (c) (d)), and 10^4 sec^{-1} for PAA and CTAB (Figs. 5 (e) (f)). Furthermore, h exhibits a steep rise at a certain critical value of V_m/b, beyond which no further increase in V_m/b is observed. This phenomenon is evident in Cases A and B for LAS(Fig. 5(c)) and AE (Fig. 5(d)) solutions, and is also observed for water (Fig. 5(a)), although its effect is small.

Figure 6 gives the results of head loss as a function of strain rate for all the test solutions flowing through the screen mesh of 300 threads per inch. It is seen that, except for the PAA solution, a unique correlation is obtained for all other solutions including water up to a strain rate of 2×10^3 sec^{-1}. Beyond this rate, the head losses for water and PEO solution become larger than those of AE, LAS and CTAB solutions at the same strain rate. The PAA solution exhibits the largest head loss over the same strain rate range. In other words, low molecular weight surfactants such as AE, LAS and CTAB show drag reduction effects compared with water, but high molecular weight

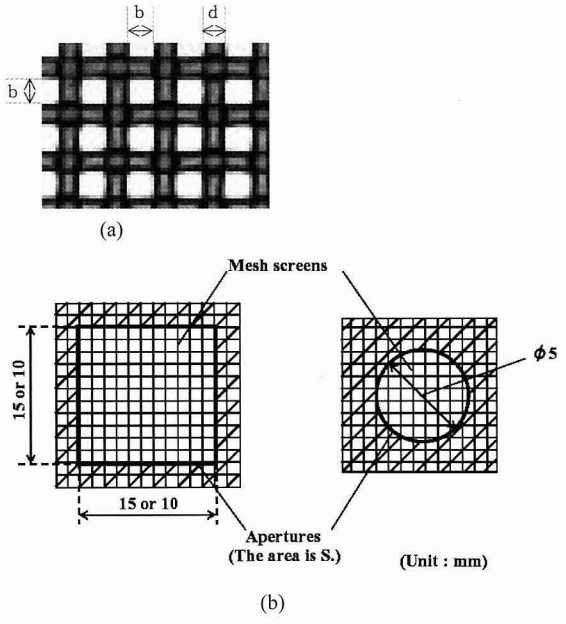

Fig. 4. (a) Photo of the screen mesh and the definition of b and d. (b) Mesh screens and the area of the apertures S.

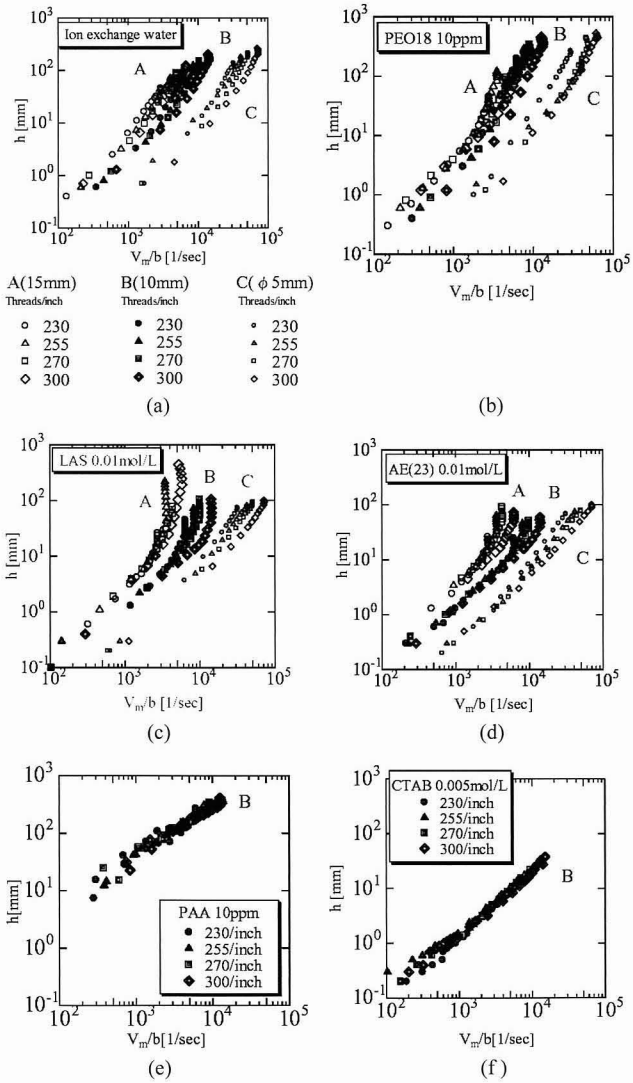

Fig. 5. Loss head h against the strain rate V_m/b for polyester mesh. (a) ion exchange water, (b) PEO18 10 ppm, (c) LAS 0.01 mol/L, (d) AE (23) 0.01 mol/L, (e) PAA 10 ppm for the case B, (f) CTAB 0.005 mol/L for the case B.

polymers like PEO and PAA, which are known to be good drag-reducing agents in turbulent flows, do not give any drag reducing effect in flow through wire mesh*, as seen in this figure. This effect is shown more clearly in Fig. 7 for the flow of the same surfactant solutions through a stainless steel 200/inch mesh.

(*)

On the PEO(18) solution, onset of drag reduction in turbulent pipe flow is at the wall shear stress $\tau_w^* \approx 0.4Pa$[9], which corresponds to the shear rate of 400 1/s. This value of shear rate is well below those of the present study except several points of very low shear rate(see Fig. 5(b)). Therefore it is thought that the molecule of PEO18 is under the condition of drag reducing if the flow is a turbulent shear flow. Furthermore, the concentration 10 ppm is high enough to generate drag reduction in turbulent pipe flows.[9,10,11] On the PAA 10 ppm solution, the large pressure loss shown in Fig. 6 is thought to be caused by the elastic stress or some vortices generated upstream of the mesh screen.[12,13]

3.1 Correlation Between Reynolds Number and Drag Coefficient

So far, flow through mesh screens has been regarded as an external flow around the threads of the mesh and the following definitions of Reynolds number and drag coefficient have been adopted[14]:

$$\text{Reynolds number: } (\mathrm{Re})_d = \frac{Ud}{\nu}, \tag{2}$$

where U is the mean velocity of the flow approaching the screen, d is the diameter of the thread weaving the screen of the square mesh and ν is the kinematic viscosity of the liquid.

$$\text{Drag coefficient: } K = \frac{2gh}{U^2}. \tag{3}$$

The following experimental correlation for air between $(\mathrm{Re})_d$ and K was proposed[14,15]:

$$K = K_\infty + \frac{55}{(\mathrm{Re})_d} \tag{4.1}$$

$$K_\infty = \left(\frac{1-0.95}{0.95\alpha}\right)^2 \tag{4.2}$$

An attempt was made to correlate the present experimental results using Eq. (4.1), as shown in Figs. 8(a) and (b) for water flowing through the 15 × 15 mm square mesh, and for AE(23) solution flowing through the circular hole of Φ 5 mm, respectively. It is evident that neither the experimental data collapse into a master curve, nor they fit with the empirical correlation for air. The present results suggest that the external flow model may not be a suitable model for the liquid mesh flow; perhaps an internal flow model may be more appropriate.

For internal flow through mesh screens, Reynolds number Re_m and drag coefficient C_{Dm} are defined as follows:

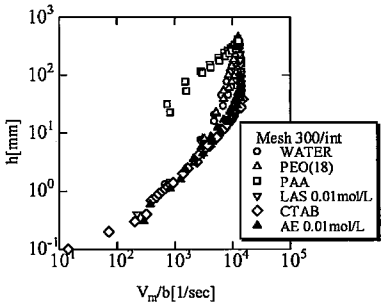

Fig. 6. h for all the solutions used for the screen mesh of 300 threads per inch(polyester mesh).

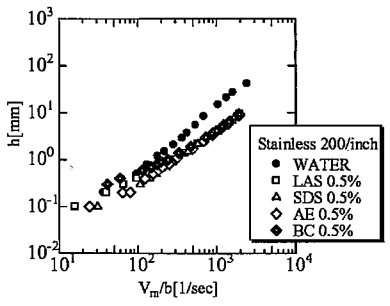

Fig. 7. h against V_m/b for the stainless mesh 200/inch.

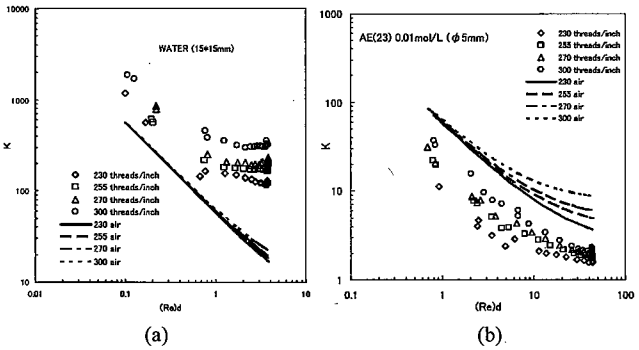

Fig. 8. Arrangement of the polyester mesh data by the relationship for air(lines). $(\mathrm{Re})_d$ is the Reynolds number given by $(\mathrm{Re})_d = \frac{Ud}{\nu}$, where U is the mean velocity of the flow approaching the screen, d is the diameter of the thread weaving the screen of the square mesh and ν is the kinematic viscosity of the liquid. K is the drag coefficient given by $K = \frac{2gh}{U^2}$. (a) water for 15 *mm* × 15 *mm* and (b) AE (23) 0.01 mol/L for ϕ 5 *mm*.

$$\mathrm{Re}_m = \frac{V_m b}{\nu} \tag{5}$$

$$C_{Dm} = \frac{h}{V_m^2/2g} \tag{6}$$

Figures 9 (a) and (b) present all experimental results for water and AE (23) solutions obtained in all three cases, A,B and C in terms of Re_m against C_{Dm}, respectively. The experimental results are seen to be well correlated for each case, irrespective of the number or the opening of the threads. However, a master curve cannot be obtained for all data because of the differences in the aperture opening S. Hence, the flow model must be refined by adopting a new set of definitions for Reynolds number and drag coefficient.

A close examination of Figs. 5(c) and (d) reveals that the steep rise in h occurs almost at the same flow rate even for different dimensions of S. This critical flow rate yields a conventional Reynolds number of 3600, calculated using the mean velocity in the inlet tube and the diameter of the inlet tube connecting to the channel. This critical Reynolds number suggests that the transition from laminar to turbulent flows in the inlet tube may influence the experimental result, or more generally, that the flow coming from the inlet tube may affect the flow upstream of the mesh screen. This conjecture was verified with a visualization experiment by injecting a color liquid upstream of the mesh screen, as shown in Fig. 10(a). It can be observed from the figure that a cylindrical column of liquid appears to be coming from the inlet tube and hitting the mesh screen. A model of the flow in the vicinity of the screen is graphically represented in Fig. 10(b).

In the flow model, it is assumed that the fluid flowing from the inlet tube into the channel does not diverge significantly, if any, and approaches the mesh screen as a liquid column of almost the same diameter (6 mm) of the inlet tube. The liquid column does not change the diameter in passing through the mesh screen of 10 × 10 mm and 15 × 15 mm apertures, but change the diameter from 6 mm to 5 mm in passing through the mesh screen of Φ 5 mm circular aperture. Based on this model, two additional velocities are further introduced. These are the velocity of the inlet tube V_t and the velocity through the mesh screen based on the liquid column of the inlet tube $V_{t,m}$. These two velocities are defined respectively by the following relationships:

$$V_t = \frac{Q}{\pi D^2/4} \tag{7}$$

$$V_{t,m} = V_t/\alpha \tag{8}$$

where D = 6 mm for the 10 × 10 mm and 15 × 15 mm apertures, and D = 5 mm for the Φ5 mm aperture. Thus, a modified Reynolds number and a modified drag coefficient are redefined as follows,

$$\mathrm{Re}_{t,m} = \frac{V_{t,m} b}{\nu} \tag{9}$$

$$C_{Dt,m} = \frac{h}{V_{t,m}^2/2g} \tag{10}$$

The experimental results shown in Fig. 9 are re-plotted in Fig. 11 using the modified Reynolds number and drag coefficient given by Eqs. (9) and (10) respectively. It is seen from Figs. 11(a-c) that all data collapse into a single master curve below a certain critical Reynolds number and are inversely proportional to the Reynolds number approximately. This kind of inverse proportionality to Reynolds number has

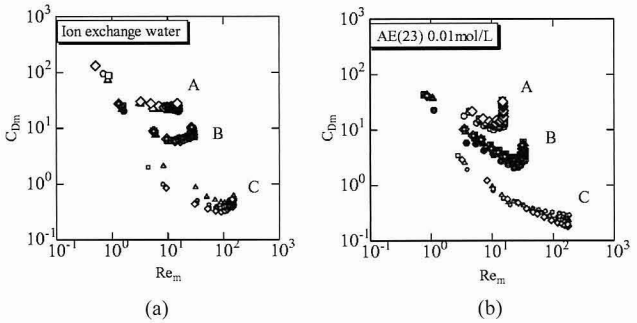

Fig. 9. Drag coefficient C_{Dm} against Reynolds number Re_m for polyester mesh. Subscript m indicates the quantities based on the mesh velocity in the opening s. (a) ion exchange water, (b) AE (23) 0.01 mol/L.

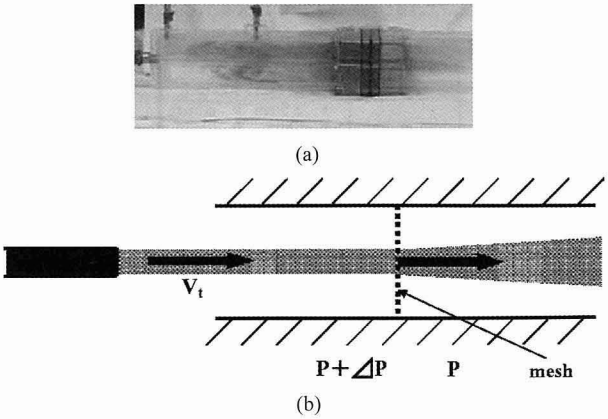

Fig. 10. (a) Photo of the liquid coming from the inlet tube and hitting the screen mesh. (b) The model representation.

been reported by several papers.[16,17,18] We see also in the figures that h increases suddenly beyond the critical Reynolds number, independent of the number of threads and the screen area S, although the critical Reynolds number is still slightly dependent on S. It appears that the proposed flow model is adequate for the flow of dilute solutions through mesh screens. It is also interesting to note, by comparing Figs. 11(b) and (c) with Fig. 11(a) that the drag coefficients obtained for the detergent solutions, AE(23) and LAS, are much lower than that obtained for water at the same Reynolds number. This indicates a drag reduction phenomenon, and surfactants such as those used in the present study are effective drag-reducers for flow through mesh screens. By contrast, PEO and PAA solutions, which are well-known drag-reducers for turbulent flow in pipes, did not manifest any drag reduction phenomenon in screen flow, as already shown in Fig. 6. Consequently, it is suggested that surfactants used as detergents promote the penetration of washing liquids into clothes by decreasing the resistance of the liquid and bring about a higher efficiency on detergency.

3.2 Drag Reduction Mechanisms

There have been many studies, both theoretical and experimental, on drag reduction in turbulent pipe flow using polymer additives. A comprehensive review on this subject can be found in a recent paper by Min, et al.[19] However, the drag reduction phenomenon observed in the present study does not correspond to any of the previous studies, because the phenomenon occurs over a Reynolds number range well below to those encountered in turbulent pipe flow, as seen in Figs. 8 and 9. This indicates that the drag reduction observed in the present study may be caused by a mechanism totally different from that observed for dilute polymer solutions in turbulent pipe flow. As seen from Fig. 5, water, PEO and all other surfactant solutions have almost the same loss head h until the strain rate V_m/b reaches around 2×10^3 sec^{-1}. Above this value of strain rate, the head losses measured for water and PEO becomes higher than those for the surfactant solutions. In other words, a drag reduction phenomenon was observed for the surfactant solutions as compared to water flow. One possible cause of the observed drag reduction is the destabilization of disturbances or eddies in the flow upstream of the mesh screen caused by the surfactant molecules. Contrary to this, it has been reported that in tubular flow, dilute PEO and HEC solutions tend to generate fluctuations prior to reaching the conventional transition from laminar to turbulent flow observed in water flow, resulting in higher pressure losses in laminar flow of dilute polymer solutions.[20,21] Another possible cause for drag reduction is the boundary slip between the surfactant solution and the solid surfaces such as the polyester and stainless steel surfaces used in the present study. Boundary slip between Newtonian liquids and substrates have been recently reported by numerous researchers.[22,23,24] However, the slip effect, although cannot be completely ruled out, is deemed not to be a main cause since the effect of the conventional slip phenomenon is much less than the present drag reduction effect. Although the drag reduction phenomenon observed for the flow of surfactant solutions through mesh screens in the present study is real, none of the conventional mechanisms proposed in literature to explain turbulent drag reduction in pipe flow applies here. It is currently believed that the drag reduction phenomenon observed here could be due to complex interactions in the interface region between the hydrophilic and lipophilic groups of the surfactant, and the substrate wall. However, further work is required to clarify the cause of drag reduction in mesh flow and to propose a plausible mechanism.

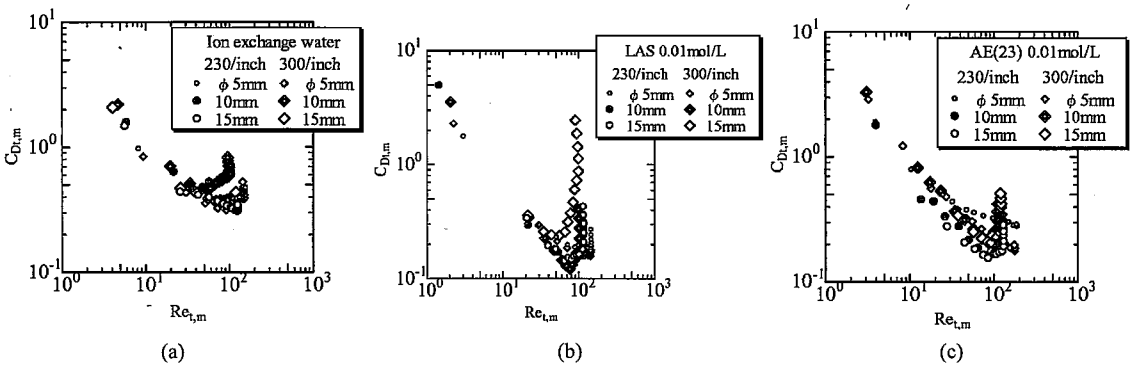

Fig. 11. $C_{Dt,m}$ against $Re_{t,m}$ for polyester mesh, where subscripts t,m mean that quantities are based on the mesh velocity calculated from the velocity of the liquid coming from the inlet tube. (a) ion exchange water, (b) LAS 0.01 mol/L, (c) AE (23) 0.01 mol/L.

4. CONCLUDING REMARKS

Pressure losses across mesh screens for the flow of water and dilute aqueous solutions of detergents and polymers were measured. It was found that solutions of low molecular weight surfactants such as AE, LAS, BC, SDS and CTAB show significant drag reduction effects compared with water, but not the high molecular weight polymers like PEO and PAA, which are well known to be good drag reducing agents in turbulent pipe flows.

The head loss over the mesh screen is greatly influenced by the conditions of the liquid upstream of the inlet. Flow visualization showed that very little divergence of the flow from the inlet to the mesh screen occurs in the channel and the liquid enters the mesh screen mainly as a liquid column of diameter similar to the inlet tube. A flow model based on this observation was proposed which yielded a good correlation of drag coefficient with Reynolds number.

Surfactants such as LAS, AE, BC and SDS are used in vast quantities in detergents. The present experimental results suggested that detergents are effective for removal of dirt stains in washing not only due to their chemical effects, but also due to the increased mobility of detergent liquids between clothing threads, as a result to its drag- reducing characteristic.

Acknowledgements

The authors wish to express many thanks to Prof. Carlos Tiu for comments and suggestions on contents and English. They gratefully acknowledge also many helps by Mr. Ryuichi Kayaba, Mr. Masahiro Karasawa and Mr. Yoshihiko Iino.

REFERENCES

1) Visser J, *J Colloid and Interface Science*, **34**, 26 (1970).
2) Gotoh K, Iriya M, Mitsui A, Tagawa E, *Colloid & Polymer Sci*, **261**, 805 (1983).
3) Tada C, *Kasei-Gaku Zasshi*, **30**, 278 (1979).
4) Hasegawa T, Tada C, *Yu-Kagaku* , **32**, 397 (1983).
5) Hasegawa T, Tada C, *Yu-Kagaku* , **34**, 545 (1985).
6) Hasegawa T, Narumi T, Konno M, Tada C, *Yu-Kagaku* , **36-67**, 4187 (1987).
7) Amaki K, Hasegawa T, Konno M, *NIHON REOROJI GAKKAISHI(J Society of Rheology, Japan)* , **21**, 41 (1993).
8) Watanabe H, Hasegawa T, Narumi T, Tamano K, *Transactions of the Japan Society of Mechanical Engineers* , **61-582**, 393 (1995).
9) Virk PS, Merrill EW, Mickley HS, Smith KA, Mollo-Christensen EL, *J Fluid Mech* , **30**, 305 (1967).
10) Goren Y, Norbury JF, *Transactions of the ASME*, 814 (1967).
11) Hasegawa T, Tomita Y, Mochimaru Y, *Bulletin of the JSME*, **15-87**, 109 (1972).
12) James DF, Acosta A J, *J Fluid Mech*, **42**, 269 (1970).
13) James DF, Saringer J H, *J Non-Newtonian Fluid Mech*, **11**, 317 (1982).
14) Ward-Smith AJ, *Internal Fluid Flow, Clarendon Press Oxford*, 463-469, (1980).
15) de Vahl Davis G, *Proc. First Australasian Conference on Hydraulics and Fluid Mechanics*, 191 (1964).
16) Roscoe R, *Philos Mag*, **440**, 338 (1949).
17) Johansen FC, *Proc Phys Soc*, **A 126**, 231 (1930).
18) Hasegawa T, Suganuma M, Watanabe H, *Phys Fluids*, **9** (1), 1 (1997).
19) Min T, Yoo J Y, Choi H, Joseph D D, *J Fluid Mech*, **486**, 213 (2003).
20) Hasegawa T, Tomita Y, Mochimaru Y, *Bulletin of the JSME*, **15-87**, 1093 (1972).
21) Hasegawa T, Tomita Y, *Bulletin of the JSME*, **17-103**, 73 (1974).
22) Watanabe K, Udagawa Y, Udagawa H, *J Fluid Mech*, **381**, 225 (1999).
23) Neto C, Evans DR, Bonaccurso E, Butt H, Craig VSJ, *A review of experimental studies Reports on Progress in Physics*, **68**, 2859 (2005).
24) Zhu Y, Granik S, *Langmuir* , **18**, 10058 (2002).